

SPECTRAL PECULIARITIES OF RADIATION OF TRAVELLING-WAVE TWO CRYSTAL OPTICAL PARAMETRIC GENERATOR *

S. Ališauskas, R. Butkus, A. Piskarskas, K. Regelskis, and V. Smilgevičius

Department of Quantum Electronics, Vilnius University, Saulėtekio 9, LT-10222 Vilnius, Lithuania

E-mail: valerijus.smilgevicius@ff.vu.lt

Received 29 June 2005

The results of theoretical and experimental investigations of two crystal travelling-wave optical parametric generator (TOPG) are presented. It is shown that the efficiency and angular structure of TOPG output depends on the distance between crystals. The experimentally observed efficiency modulation is attributed to air dispersion and this is confirmed by theoretical calculations.

Keywords: nonlinear optics, optical parametric generation

PACS: 42.65.Yj

1. Introduction

Picosecond and femtosecond travelling-wave optical parametric generators (TOPG) are widely used in various spectroscopic experiments as tunable light sources. The single crystal TOPG generates very wide spectrum determined by noncollinear phase-matching conditions in nonlinear crystal and characterized by specific angular–frequency distribution [1, 2]. Spectrum selection using the two crystal scheme TOPG was proposed in Refs. [3, 4] in 1974 and the detailed overview of picosecond and femtosecond travelling-wave parametric generators was presented in [5]. In two crystal scheme, the first TOPG crystal generates broadband spectrum and the second crystal is used to amplify only the spectral components with propagation directions lying within the pump beam propagation angle. The spectrum narrowing depends on the distance between crystals; by increasing the distance, angular filtering allows to decrease the spectral width and divergence of TOPG output and to smooth the spatial and spectral distributions [1]. On the other hand, for effective parametric amplification in the second crystal it is necessary that the phases of interacting pump, signal, and idler waves were such that $\varphi_1 + \varphi_2 - \varphi_3 = -\pi/2$,

where $\varphi_1, \varphi_2, \varphi_3$ are the phases of signal, idler, and pump waves, respectively.

This phenomenon was used for mode-locking CW lasers by nonlinear mirror [6]. Nonlinear frequency converter consisting of nonlinear crystal and dichroic mirror inside the CW laser cavity operate as nonlinear mirror mode-locker. The second harmonic (SH) generated in a nonlinear crystal and the fundamental (FH) beams are returned by dichroic mirror back into nonlinear crystal. If the phase difference between SH and FH beams is $\theta = 2\varphi_1 - \varphi_2 = -\pi/2$, or differs from it by $2\pi m$ (m is an integer), the FH radiation will grow in the nonlinear crystal at the expense of the SH beam, the optical parametric amplification will be realized. Using this technique the mode-locking operation for Nd:YAG active laser media was repeatable at 6.5 cm distance between the nonlinear crystal and the dichroic mirror. At this distance the phase difference changed by π due to air dispersion of SH and FH waves [7].

Another approach to this phenomenon was implemented in simultaneous wavelength conversion and amplitude modulation in a periodically poled lithium niobate crystal consisting of two poled sections containing an unpoled dispersion section in between [8]. The difference is that not the air but the material dispersion is utilized. The SH is generated in the crystal but since the second poled section is rotated with respect to the first one, by moving the crystal in the

* The report presented at the 36th Lithuanian National Physics Conference, 16–18 June 2005, Vilnius, Lithuania.

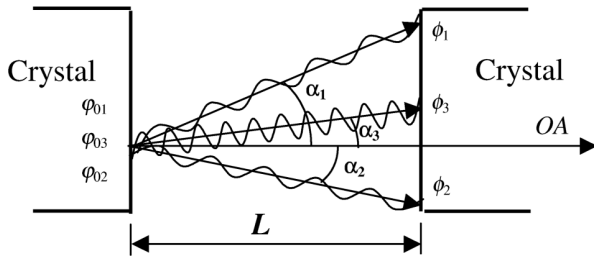


Fig. 1. Schema of two crystal travelling-wave optical parametric generator.

transverse direction one can change the amount of unpoled material in the path of laser radiation. Thus, the relative phase between the fundamental and SH waves can be controlled resulting in modulation of SH amplitude. However, in the cases mentioned above, the output wavelength is fixed.

In this paper we present the results of investigation of two crystal tunable travelling-wave optical parametric generator including the analysis of influence of air dispersion between OPG crystals.

2. Theory

In our calculations we used TOPG consisting of two nonlinear crystals separated by a distance L (see Fig. 1). In our considerations we take into account that between the nonlinear crystals there is air with dispersion properties presented in [9]. For theoretical analysis we use the geometrical representation, neglecting the diffraction. Also, we assume that the surfaces of crystals are parallel and perpendicular to the optical axis (OA in Fig. 1).

At the output of the first crystal, for optimal three-wave parametric interaction, the generalized phase is equal to

$$\varphi_0 = \varphi_{03} - \varphi_{01} - \varphi_{02}, \tag{1}$$

where φ_{01} , φ_{02} , and φ_{03} are the phases of the signal, idler, and pump waves, respectively. Optical path for each wave propagating from the output surface of the first crystal to the input surface of the second crystal depends on deviation from optical axis OA and on air refractive index. So, acquired phase shift of each wave is equal to

$$\varphi_i = 2\pi \frac{n_i^{\text{air}}}{\lambda_i} \frac{L}{\cos \alpha_i} = k_i^{\text{air}} \frac{L}{\cos \alpha_i}, \tag{2}$$

$i = 1, 2, 3$ (indices 1, 2, 3 correspond to signal, idler, and pump beams, respectively). n_i^{air} is the refractive index of air, α_i is wave deviation from optical axis, and

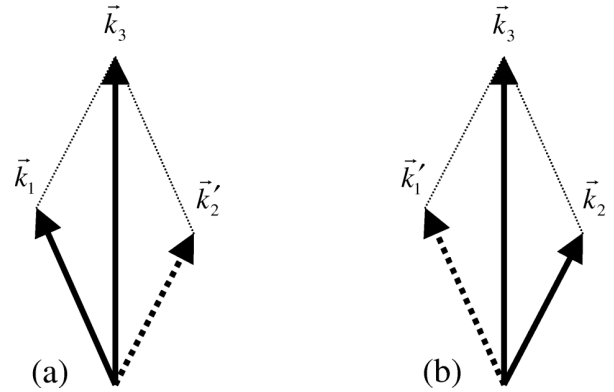


Fig. 2. In the second crystal, as a consequence of interaction of pump wave k_3 with (a) signal k_1 and (b) idler k_2 waves, a pair of conjugate waves k'_2 and k'_1 is produced.

$k_i^{\text{air}} = 2\pi n_i^{\text{air}}/\lambda_i$. The phase difference acquired between waves due to propagation from the first to the second crystal is given by

$$\begin{aligned} \varphi &= \varphi_3 - \varphi_1 - \varphi_2 \\ &= \left(\frac{k_3^{\text{air}}}{\cos \alpha_3} - \frac{k_1^{\text{air}}}{\cos \alpha_1} - \frac{k_2^{\text{air}}}{\cos \alpha_2} \right) L. \end{aligned} \tag{3}$$

The last expression represents the phase mismatch between pump, signal, and idler waves and, as mentioned above, it depends on deviation from optical axis and on air refractive index dispersion. The optical parametric amplification in the second crystal decreases if $\varphi \neq 0$.

Wavelengths and deviation angles α_i of the signal, idler, and pump waves are related by phase-matching condition. Using phase-matching angles the deviation angles from optical axis can be expressed in this way: $\alpha_1 = \gamma - \theta_1$, $\alpha_2 = \gamma - \theta_2$, $\alpha_3 = \gamma - \theta_3$, where θ_1 , θ_2 , θ_3 are external phase-matching angles and γ is the angle between crystal optical axis and optical axis OA.

So, at the input of the second crystal the phases for signal, idler, and pump waves are

$$\phi_1 = \varphi_{01} + \varphi_1, \tag{4a}$$

$$\phi_2 = \varphi_{02} + \varphi_2, \tag{4b}$$

$$\phi_3 = \varphi_{03} + \varphi_3. \tag{4c}$$

The phase alone of an individual wave might not have relevant meaning, but later it will be cancelled out. In the second crystal, as a consequence of interaction of pump wave k_3 with signal k_1 and idler k_2 waves, a pair of conjugate waves k'_2 and k'_1 are produced (see Fig. 2(a, b)). The signal and idler waves can be amplified or attenuated depending on the phase differences between waves k_1 , k_2 and conjugated waves

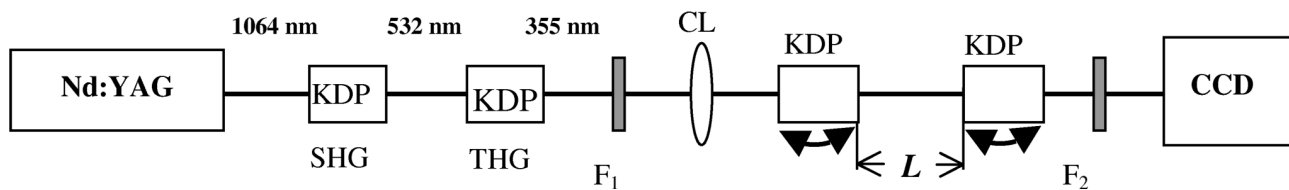


Fig. 3. Experimental set-up. Nd:YAG is picosecond Nd:YAG laser and amplifier, SHG is second harmonic generation, THG is third harmonic generation, KDP are nonlinear KH_2PO_4 crystals for the second, the third harmonic generation, and optical parametric generation, F1 and F2 are filters, CL is cylindrical lens, CCD is charge coupled device for registering intensity distributions.

k'_1 , k'_2 , respectively. Thus, the waves keeping phases $\phi_1 = \varphi_{01} + \varphi_1$ and $\phi_3 = \varphi_{03} + \varphi_3$ produce the conjugated wave with a phase

$$\phi'_2 = (\varphi_{03} + \varphi_3) - (\varphi_{01} + \varphi_1) - \varphi'_0, \quad (5)$$

where φ'_0 is the generalized phase of the three-wave parametric amplification. Analogically, waves with the phases $\phi_2 = \varphi_{02} + \varphi_2$ and $\phi_3 = \varphi_{03} + \varphi_3$ produce another conjugated wave having the phase

$$\phi'_1 = (\varphi_{03} + \varphi_3) - (\varphi_{02} + \varphi_2) - \varphi'_0. \quad (6)$$

Generalized phase φ'_0 used in Eqs. (5) and (6) is equal to the initial phase difference φ_0 at the output boundary of the first crystal (Eq. (1)). Or they can differ only by an integer multiple of 2π . Reducing it we can take $\varphi'_0 = \varphi_0$.

Using Eq. (4a), Eq. (6), and $\varphi'_0 = \varphi_0$, the phase difference between signal waves k_1 and k'_1 is equal to

$$\phi'_1 - \phi_1 = \varphi_3 - \varphi_1 - \varphi_2 = \varphi. \quad (7)$$

The phase difference between idler waves k_2 and k'_2 using Eqs. (4b) and (5) is

$$\phi'_2 - \phi_2 = \varphi_3 - \varphi_1 - \varphi_2 = \varphi. \quad (8)$$

As one can see, the phase difference for signal or idler waves is equal to the phase difference acquired between waves due propagation from the first till the second crystal (Eq. (3)). Pairs of the waves k_1 and k'_1 or k_2 and k'_2 are equal in their wavelengths and propagation directions ($\vec{k}_1 = \vec{k}'_1$ and $\vec{k}_2 = \vec{k}'_2$). They differ only in their phases. In the second crystal the signal wave k_1 with initial amplitude A_{01} is amplified η_1 times. At the output of the crystal the amplitude of the amplified signal wave is equal to $\eta_1 A_{01}$ and the amplitude of corresponding conjugate idler wave is equal to $(\eta_1 - 1)(\omega_2/\omega_1)^{1/2} A_{01}$. Here $\omega = 2\pi c/\lambda$ is an angular frequency of a wave. Analogically, the idler wave k_2 with initial amplitude A_{02} is amplified η_2 times and at the output of the second crystal the amplitude of the amplified idler wave is equal to $\eta_2 A_{02}$ while the amplitude of corresponding conjugate signal wave is equal to

$(\eta_2 - 1)(\omega_1/\omega_2)^{1/2} A_{02}$. Hence, these waves reciprocally collinearly interfere and the intensity distributions for signal and idler waves correspondingly are

$$I_1 = \eta_1^2 A_{01}^2 + (\eta_2 - 1)^2 \frac{\omega_1}{\omega_2} A_{02}^2 + 2A_{01}A_{02} \sqrt{\frac{\omega_1}{\omega_2}} \eta_1 (\eta_2 - 1) \cos \varphi, \quad (9a)$$

$$I_2 = \eta_2^2 A_{02}^2 + (\eta_1 - 1)^2 \frac{\omega_2}{\omega_1} A_{01}^2 + 2A_{02}A_{01} \sqrt{\frac{\omega_2}{\omega_1}} \eta_2 (\eta_1 - 1) \cos \varphi. \quad (9b)$$

Let us assume that $A_{01}^2/\omega_1 = A_{02}^2/\omega_2$ (equal number of signal and idler photons at the input of the second crystal) and $\eta_1 = \eta_2 = \eta \gg 1$. Then, using Eqs. (9a) and (9b), the intensity distributions for signal and idler waves are

$$I_1 = 2\eta^2 A_{01}^2 (1 + \cos \varphi) = \eta^2 \frac{\omega_1}{\omega_2} A_{02}^2 (1 + \cos \varphi), \quad (10a)$$

$$I_2 = 2\eta^2 A_{02}^2 (1 + \cos \varphi) = \eta^2 \frac{\omega_2}{\omega_1} A_{01}^2 (1 + \cos \varphi). \quad (10b)$$

As one can see, the intensities of signal and idler waves strongly depend on the phase mismatch φ (see Eq. (3)). In the central part of the intensity distribution (deviation angle α_i is equal to zero there, thus Eq. (3) can be written as $\varphi = (k_3^{\text{air}} - k_1^{\text{air}} - k_2^{\text{air}}) L = \Delta k^{\text{air}} L$), the intensity of a particular wave depends only on the distance L between two crystals. On the other hand, for the different deviation angles α at the fixed distance L between two crystals, angular intensity modulation is present for the signal and idler waves.

Attention should be drawn to a special case when the amplitude of one of the waves (signal or idler) at the entrance of the second crystal is equal to zero. For instance, the idler wave can be blocked ($A_{02} = 0$) by

inserting a filter between the crystals, which is transparent only for the pump and signal waves. In this case, using Eqs. (9a) and (9b), the intensity distributions are

$$I_1 = \eta_1^2 A_{01}^2, \quad (11a)$$

$$I_2 = (\eta_1 - 1)^2 \frac{\omega_2}{\omega_1} A_{01}^2. \quad (11b)$$

Obviously, there is no dependence on the phase mismatch φ .

At vanishing air dispersion between two crystals (e. g. vacuum between crystals), the phase mismatch is zero for collinear interaction and the intensity is maximum in the central part of the beam.

3. Experiment

The experimental set-up is presented in Fig. 3. The picosecond Nd:YAG laser system (mode-locked oscillator with regenerative amplifier) was used as a pump source for TOPG, where type I interaction was realized. Spectrum and intensity distribution formation peculiarities in two KDP (KH_2PO_4) crystal TOPG were investigated. The third harmonic radiation was separated from fundamental and the second harmonic radiation by a filter F1 and focussed onto the TOPG crystals by a cylindrical lens with a focal length of 1 m. The second crystal was placed in the focus of the lens while the first crystal was placed before the focus. Both crystals were 6 cm long. The first TOPG crystal was mounted on the delay line for changing the distance between TOPG crystals. Both crystals were angle-tuned for desired wavelength and the intensity distributions of TOPG output in the far field were registered with a CCD camera. The dependence of normalized intensity of amplified in the second crystal signal wave ($\lambda = 591$ nm) on the distance between TOPG crystals and the theoretical fit derived after substituting Eq. (3) into (10) is depicted in Fig. 4. The intensity was measured in the central part of the signal wave. It is clearly seen that intensity reaches its maximum when the distance between the TOPG crystals is a multiple of ~ 37 mm. Obviously, the first maximum occurs when no air is present between the crystals. Intensity minima are located in between the maxima, within equivalent distances. It must be noted that periodicity of intensity maxima depends on the wavelengths of interacting waves: it is lowest at degeneracy and gets higher when detuning away from it (see Fig. 5). As can be seen, experimental results are in good agreement with theoretical fit. Spatial-angular distribution of two crystal TOPG output also depends

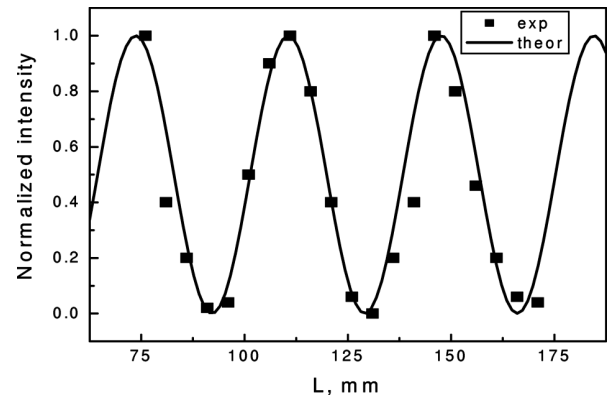


Fig. 4. Dependence of normalized intensity of the generated signal wave on the distance L between crystals (signal wavelength $\lambda = 591$ nm). Squared dots represent measured data and solid curve is theoretical fit.

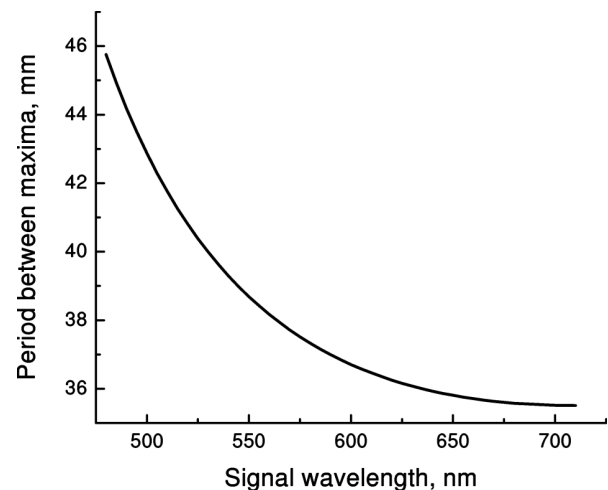
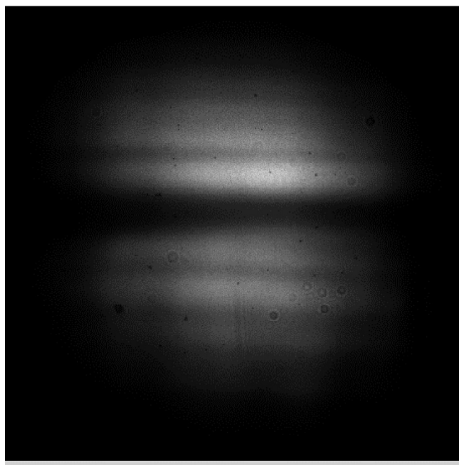
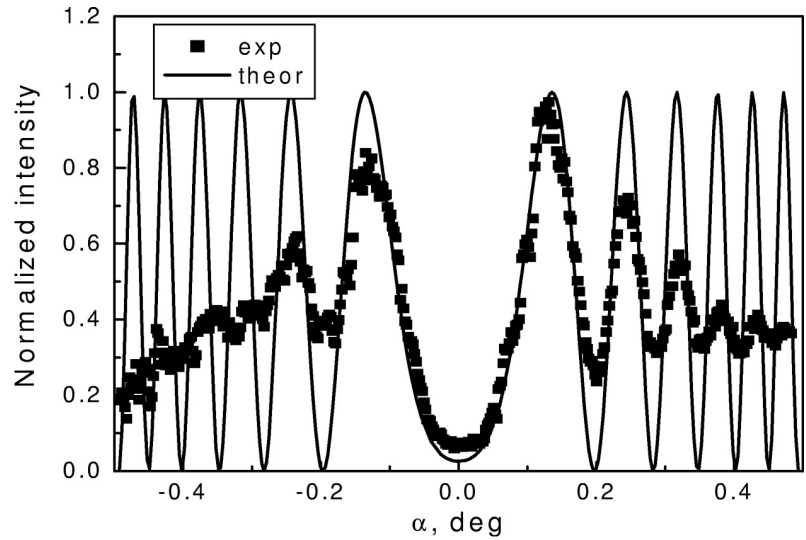


Fig. 5. Variation of period between intensity maxima in the central part on signal wavelength for pump wavelength of 355 nm.

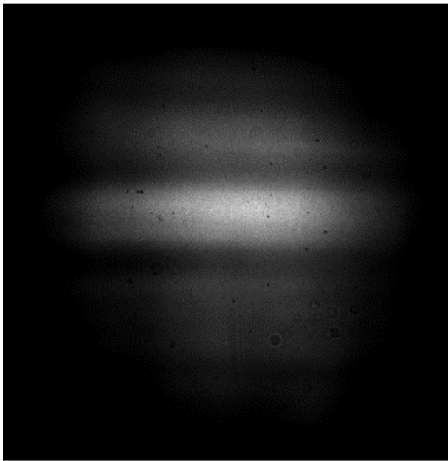
on the distance between crystals. It consists of multiple alternating maxima and minima with central part setting the pace and edges following it. For every maxima of the intensity distribution the phase mismatch φ (see Eq. (3)) is an integer multiple of 2π and for every minima the phase mismatch is $2\pi(n + 1/2)$ (with $n = 0, \pm 1, \pm 2, \dots$). The minimum central part corresponds to the case when phase mismatch for collinearly propagating waves is $2\pi(n + 1/2)$. Figure 6 presents (a) angular intensity distribution and (b) its radial distribution of a signal wave ($\lambda = 632$ nm) with the minimum central part surrounded by maxima and so forth. If phase mismatch for collinearly propagating waves is multiple of $2\pi n$, the intensity in the central part is maximum. In this case, angular intensity distribution and its radial distribution with a theoretical fit are depicted in Fig. 6(c, d). The theoretical fits are presented in Fig. 6(b, d). One can note the decreasing period



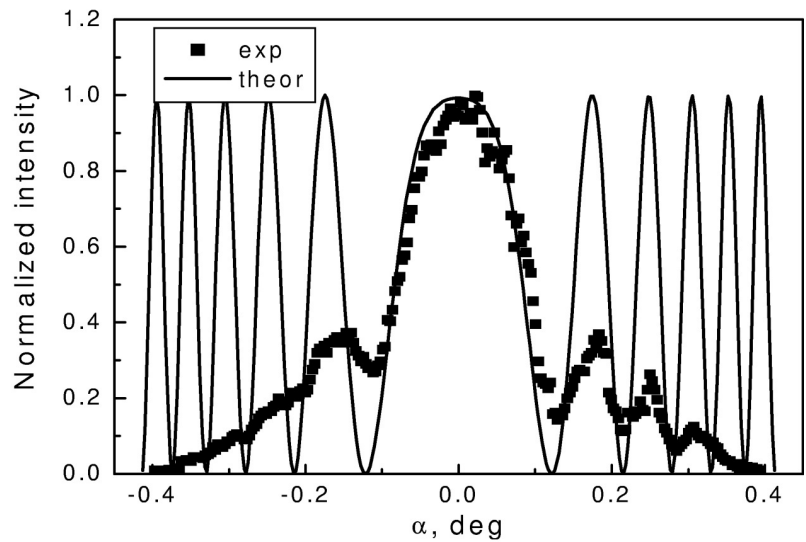
(a)



(b)



(c)



(d)

Fig. 6. (a) Angular intensity distribution and (b) its radial distribution of TOPG output radiation ($\lambda = 632 \text{ nm}$) for non-optimal distance between crystals ($L = (n + 1/2) \times 36 \text{ mm}$, $n = 0, 1, 2, \dots$); (c) angular intensity distribution and (d) its radial distribution of TOPG output radiation for optimal distance between crystals ($L = n \times 36 \text{ mm}$, $n = 0, 1, 2, \dots$). Experimental results (filled squares) well correspond to theoretical calculations (solid lines).

between maxima while moving away from the central part.

4. Conclusion

It is shown that in two crystal TOPG the intensity distribution depends on the distance between crystals and the conversion efficiency is the highest when the phase difference among pump, signal, and idler waves acquired by propagating through the air gap between the crystals satisfy the requirement $\varphi = 2\pi n$, with n being integer number. In designing the travelling-wave

optical parametric generators, it is crucial to take the air dispersion into account, however, air dispersion is negligible if only one of the two parametrically generated waves is seeded into the second nonlinear crystal.

Acknowledgements

This work was supported by EU LASERLAB-EUROPE project and the Lithuanian State Science and Studies Foundation, project No. V-05032.

References

- [1] H. Bergner, V. Brückner, and B. Schröder, Investigation of temporal and spectral properties of ultrashort light pulses from an optical parametric amplifier, *Opt. Acta* **29**, 1491–1502 (1982).
- [2] B. Schröder, Frequency characteristic and spatial intensity distribution of light generated and amplified three-photon interaction, *Opt. Commun.* **49**, 75–78 (1984).
- [3] A.H. Kung, Generation of tunable picosecond VUV radiation, *Appl. Phys. Lett.* **25**, 653–654 (1974).
- [4] A. Laubereau, L. Greiter, and W. Kaiser, Intense tunable picosecond pulses in the infrared, *Appl. Phys. Lett.* **25**, 87–89 (1974).
- [5] R. Danielius, A. Piskarskas, A. Stabinis, G.P. Banfi, P. Di Trapani, and R. Righini, Travelling-wave parametric generation of widely tunable, highly coherent femtosecond light pulses, *J. Opt. Soc. Am. B* **10**, 2222–2232 (1993).
- [6] K.A. Stankov and J. Jethwa, A new mode-locking technique using a nonlinear mirror, *Opt. Commun.* **66**, 41–46 (1988).
- [7] K.A. Stankov, A mirror with an intensity-dependent reflection coefficient, *Appl. Phys. B* **45**, 191–195 (1988).
- [8] K.W. Chang, A.C. Chiang, T.C. Lin, B.C. Wong, Y.H. Chen, and Y.C. Huang, Simultaneous wavelength conversion and amplitude modulation in a monolithic periodically-poled lithium niobate, *Opt. Commun.* **203**, 163–168 (2002).
- [9] B. Edlen, The refractive index of air, *Metrologia* **2**, 71–80 (1966).

DVIEJŲ KRISTALŲ BĖGANČIOS BANGOS PARAMETRINIO ŠVIESOS GENERATORIAUS SPINDULIUOTĖS SPEKTRINIAI YPATUMAI

S. Ališauskas, R. Butkus, A. Piskarskas, K. Regelskis, V. Smilgevičius

^a *Vilniaus universitetas, Vilnius, Lietuva*

Santrauka

Pateikti dviejų KDP (KH₂PO₄) kristalų bėgančios bangos parametrinio šviesos generatoriaus (PŠG) spinduliuotės spektrinių tyrimų ypatumai. Pirmajame kristale žadinama parametrinė šviesos superluminescencija buvo stiprinama antrajame kristale. Dėl oro dispersijos į antrąjį kristalą patekusių bangų (kaupinimo, signalo ir skirtuminės bangos) fazės priklauso nuo atstumo tarp kristalų.

Ekspimentiniais tyrimais parodyta, kad dviejų kristalų bėgančios bangos PŠG efektyvumas ir generuojamo pluošto intensyvumo skirstinio sandara priklauso nuo atstumo tarp kristalų. Tokį erdvinį skirstinį lemia trijų bangų fazinis išderinimas, kuris pasireiškia dėl nevienodų optinių kelių sklindant signalinei, šalutinei ir kaupinimo bangoms tarp kristalų.